

Reduction of Altitude Diffuser Jet Noise Using Water Injection

Daniel C. Allgood
NASA Stennis Space Center
John C. Stennis Space Center, MS 39529

Grady P. Saunders
Jacobs Technology Inc.
Tullahoma, TN 37388

Lester A. Langford
Lockheed Martin Inc.
John C. Stennis Space Center, MS 39529

A feasibility study on the effects of injecting water into the exhaust plume of an altitude rocket diffuser for the purpose of reducing the far-field acoustic noise has been performed. Water injection design parameters such as axial placement, angle of injection, diameter of injectors, and mass flow rate of water have been systematically varied during the operation of a subscale altitude test facility. The changes in acoustic far-field noise were measured with an array of free-field microphones in order to quantify the effects of the water injection on overall sound pressure level spectra and directivity. The results showed significant reductions in noise levels were possible with optimum conditions corresponding to water injection at or just upstream of the exit plane of the diffuser. Increasing the angle and mass flow rate of water injection also showed improvements in noise reduction. However, a limit on the maximum water flow rate existed as too large of flow rate could result in un-starting the supersonic diffuser.

Nomenclature

| | | |
|-----------|---|--|
| D_{DE} | = | exit diameter of altitude diffuser |
| D_{WJ} | = | diameter of noise suppressor water jets |
| J | = | momentum flux ratio of a single water jet to the altitude diffuser exhaust jet |
| OSPL | = | overall sound pressure level, dB (reference pressure = 20e-6 Pa) |
| r | = | radial location |
| SDT | = | sub-scale diffuser test facility |
| V_{WJi} | = | exit velocity of an individual water jet from the noise suppressor |
| V_{SDT} | = | exit velocity of SDT altitude diffuser |
| W_{A3} | = | total mass (weight) flow rate of A-3 altitude diffuser |
| W_{SDT} | = | total mass (weight) flow rate of SDT altitude diffuser |
| W_{WJ} | = | total mass (weight) flow rate of water jets |
| x | = | axial location |
| ρ | = | density |

I. Introduction

A. A-3 and SDT Altitude Test Facilities

NASA John C. Stennis Space Center (NASA-SSC) has recently constructed the A-3 altitude test facility for development and certification testing of the J-2X LOX/LH2 engine. The 300,000 lbf J-2X engine was originally designed to serve as the earth departure stage for the ARES V vehicle and the upper-stage of the ARES I vehicle. A critical test requirement for the J-2X engine was that it be tested under start/re-start conditions of 100,000 ft (or 0.16psia) simulated altitude. In addition, the A-3 altitude test facility had to be capable of testing the J-2X engine in both non-gimbaled and gimbaled configurations while simulating its entire mission thrust profile, which lasted approximately 500 seconds.

The A-3 altitude test stand, depicted in Figure 1, is a very unique facility. It is roughly a 300 ft vertical test stand composed of a steel lattice structure. The structure holds the propellant delivery system, test cell and a 360 ft long diffuser. An array of 27 chemical steam generators provides the driving medium for a two-stage, superheated-steam ejector system that at nominal design conditions should effectively pump the test cell down to 0.16 psia prior to engine start. The total flow rate of steam is of the order of 5000 lbm/sec.

Due to the mission-criticality of having a reliable and successful A-3 facility, a sub-scale diffuser test facility (SDT), shown in Figure 2, was built and tested at the NASA-SSC E-Complex7. The subscale facility was designed such that it was aerodynamically similar to that of the full-scale A-3 facility. This test program was a risk mitigation effort to verify engineering predictions, provide test operation experience and pinpoint any potential design flaws prior to construction of the full-scale A-3 facility. In addition to A-3 design performance concerns, it was imperative that NASA-SSC have a complete understanding of the expected far-field acoustic signature from the A-3 test facility due to its orientation and close proximity to populated areas and highways. However, after reviewing the available acoustic data from large-scale rocket testing, there was little to no information for test facilities of this type. Furthermore, the rocket acoustic modeling tools that were available had not been formally validated for the steam-laded and relatively slower A-3 exhaust plume. This possible deficiency and uncertainty in modeling led to an effort of performing a combined experimental and computational study of the aero-acoustics from the dynamically-similar sub-scale altitude test facility. One of the primary objectives of this earlier effort was to develop a validated methodology for characterizing the far-field acoustic signature from an altitude rocket test facility of this type. The findings from this study were presented recently in a series of papers at the AIAA Joint Propulsion Conference46. However, the focus of the current report is to document additional testing that was conducted using the sub-scale facility to provide guidance on noise mitigation methodologies that might need to be implemented for A-3. The main noise mitigation technique investigated was high velocity water injected in the diffuser exhaust plume. Later sections of this report will discuss the experimental setup, the various parameters defined by the test matrix, and the results obtained from the experimental study.



Figure 1: Conceptual Rendering of the New A-3 Test Facility at NASA Stennis Space Center

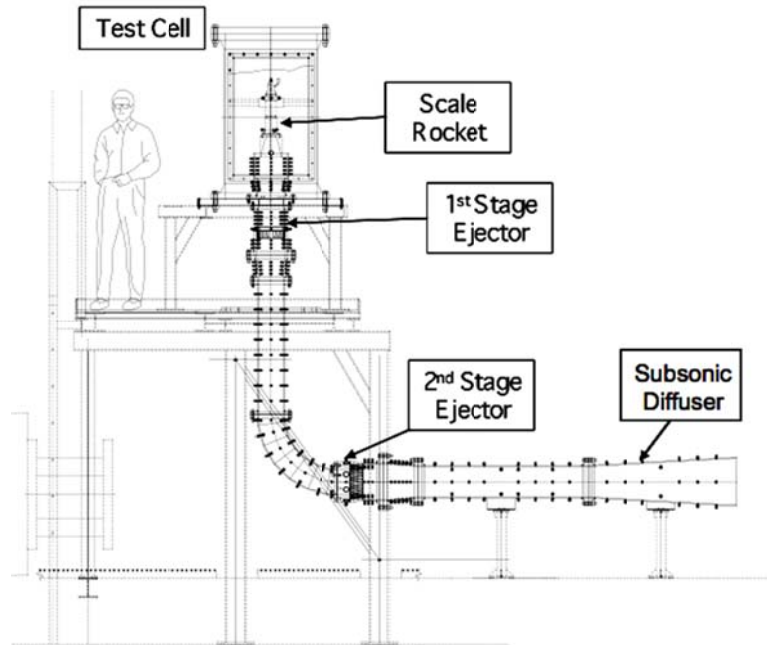


Figure 2: Sub-scale Altitude Test Facility (SDT)

B. Supersonic Jet Noise and Water-Injection Mitigation

It is generally accepted that there are three categories of supersonic jet noise: broadband shock noise, screech tones and turbulent mixing noise⁸. The first two categories occur only in supersonic jets, while the last category is present in both subsonic and supersonic jets but can have different mechanisms. In the case of an imperfectly expanded supersonic jet, a repeating pattern of shock-cell structures form in the exhaust plume. Natural flow instability waves that develop in the jet shear-layer interact with the jet shock-cell structures creating broadband shock noise. The acoustic energy generated by this noise source is primarily directed upstream. In certain cases, a feedback mechanism can occur where acoustic waves formed by the interaction of flow instabilities with the shock-cell structures reflect back upstream causing new disturbances to form at the jet nozzle lip thereby completing the feedback loop. Unlike broadband shock noise, this noise mechanism is characterized by a narrowband peak of energy in the acoustic spectrum, which is commonly referred to as “screech” tones.

The last category of supersonic jet noise is turbulent mixing noise. Turbulent mixing noise can be generated by either small or large-scale turbulent flow structures. The level and type of noise produced is dependent on the jet Mach number and temperature, and appears to be composed of three major components⁹. The first turbulent mixing noise component in a supersonic jet is Mach wave radiation generated by small turbulent eddies convecting at supersonic speeds. Small-scale eddies which form very close to the jet nozzle exit can produce coherent, high-frequency (short wavelength) Mach waves that emanate in a direction governed by the disturbance convective velocity and atmospheric speed of sound⁹. Also, supersonic-convecting large-scale eddies that form near the end of the potential core and downstream can produce Mach-waves of significantly higher strength than those produced by smaller-scale eddies, and as such are a major component of the far-field acoustic signature of an imperfectly expanded supersonic jet⁸⁻⁹. Propagation of the acoustic energy created by large-scale eddies is controlled by refraction of sound in the shear layer and as such is primarily directed downstream at some angle off the centerline of the jet¹⁰. This behavior causes the characteristic “butter-fly” pattern observed in the far-field overall sound pressure level directivity mappings of rocket engines¹¹⁻¹⁴. In addition to Mach wave radiation, turbulent mixing noise in a supersonic jet is composed of fine-scale mixing noise as seen in subsonic jets. This component of mixing noise is a result of unsteady motion of fine-scale turbulent

structures and is characterized by broadband acoustic energy due to their random or chaotic motion. The principal directivity of this noise component is at angles normal to the jet plume.

A common method of reducing rocket engine jet noise is to spray or inject a fluid into the exhaust plume. The objective is to break-up or more rapidly disperse the exhaust plume thereby reducing the noise production. Air injection, or “fluidic-chevrons”, has been successfully shown to provide a means of attenuating jet noise from air-breathing engines. However, water injection is particularly common during static testing of large-scale rocket engines as it not only provides acoustic suppression, the water also provides cooling of the exhaust plume and facility structures. There have been many fundamental studies on investigating the physics by which water injection suppresses high-speed jet noise^{9,15-16}. Some of the key findings of these studies will be outlined here as they will prove to be relevant to the current research effort. First, Krothapalli et al showed that proper injection of a small amount of water (12-16%) into the shear-layer of a hot, supersonic jet significantly reduces the velocity fluctuations, turbulent shear stresses and large-scale motions in the jet (flapping)⁹. Since a significant component of supersonic jet noise is turbulent mixing noise, this constituted in an overall sound pressure level (OSPL) reduction as high as 6dB. Their study also showed the most effective reduction in noise was obtained by injecting the water near the nozzle exit plane rather than further downstream in the mixing zone. Also, having a more normal injection of water (60 degrees relative to the jet centerline) into the exhaust plume gave a better reduction in noise. Lastly, they demonstrated that increasing the flowrate of water injection increased the noise suppression at all frequency ranges.

Norum et al have also published an in-depth study on suppressing supersonic jet noise with water injection¹⁵. In their study, they showed not only does water injection suppress turbulent mixing noise, it will also suppress shock noise by disrupting the positive phase relationship between the jet shock cells and the acoustic waves. Norum also confirmed the findings of Krothapalli et al, that acoustic attenuation is optimum when the water is injected close to the nozzle exit plane rather than further downstream. In addition to these consistent observations, Norum observed better response with less number of water injection holes delivering the same water mass flow rate. This perceived inconsistency was reconciled by Norum when he suggested that the higher injection pressures with the fewer number of water injection holes improves the sound suppression by improving jet penetration. The major scaling parameter however is probably not the injection pressure but rather the mass or momentum ratio of the water injection to exhaust flow as was suggested by Callender¹⁶ in his fluidic-injection study on reducing jet noise from turbofan engines. This and other important scaling parameters have been discussed further in the analytical paper presented by Kandula¹⁷. Kandula suggests that as the mass flow rate of water increases above 0.05-0.1, the sound suppression mechanism of water injection changes from (a) reducing turbulence levels to (b) reducing the exhaust plume mean velocity and temperature via momentum/heat transfer with the water.

The current work presents a study on the use of discrete water-jet injection for the suppression of jet noise from altitude rocket test facilities. The application of water-injection into an altitude diffuser exhaust plume for noise reduction is somewhat unique in that the water-injection has the potential to adversely affect the supersonic diffuser performance. The effects of various possible design parameters such as axial location of injection, angle of injection, number of injectors and relative flow rates on the far-field acoustic directivity as well as the diffuser performance are discussed below.

II. Experimental Facility

C. Subscale Diffuser Test Facility (SDT)

To help minimize risk of failure and limit re-design costs for the new A-3 altitude test facility, a subscale altitude facility was designed and constructed to perform a series of verification tests. These verification tests could potentially pinpoint design and/or operational issues with the A-3 test stand prior to its construction. The subscale diffuser test (SDT) facility, shown in Figure 2, is approximately 1/17th geometric scale of the A-3 test facility. A subscale J-2X engine was constructed and installed in the test facility. The area ratios, combustion chamber pressure and mixture fractions of the J-2X have been

maintained in the subscale engine. As a result, the subscale engine plume entering the diffuser closely resembles that of the J-2X. The mass flow rates of the 1st and 2nd steam ejectors have also been appropriately scaled (by square-root of mass-flow ratio) to ensure the same gas dynamic processes are occurring inside the subscale diffuser flow path. The use of the square-root of mass-flow ratio as an appropriate scale factor can be verified by looking at the definition of mass flow rate and substituting the geometric scale factor. A table comparing the full-scale A-3 design flow rates to the SDT is given in Table 1 below.

Table 1: Comparison of Design Mass Flow Rates of A-3 and SDT Altitude Facilities

| | Full-Scale | Sub-Scale | Square Root of the Ratio of Mass Flow Rates (W_{SDT}/W_{A3}) ^{0.5} |
|---|------------|-----------|--|
| Ratio of 1 st Stage Ejector to Rocket Mass Flow Rates | 0.74 | 0.69 | - |
| Ratio of 2 nd to 1 st Stage Ejector Mass Flow Rates | 9.0 | 9.0 | - |
| Total Mass Flow Rate (lbm/sec) | 5448 | 17.16 | 1/17.82 |
| <i>Geometric Scale Factor = 1/17</i> | | | |

In addition, to facilitate monitoring the performance of the SDT, the subscale diffuser has been instrumented with an array of high-speed pressure transducers and thermal couples to assess the facility operation behavior and efficiency. The high-speed diffuser data in conjunction with IR outer wall surface temperature measurements also provided experimental data to assess the capability of the CFD simulations in capturing the locally averaged flow and heat transfer characteristics throughout the diffuser flow path.

D. Acoustic Measurements and Data Collection

In order to anchor far-field acoustic models that were being using to estimate the full-scale A-3 test facility acoustic signature, a detailed acoustic mapping of the subscale test facility during its operation was performed. A radial arc of seven free-field microphones (B&K ½” Type 4191) was placed in what was perceived a priori to be the acoustic far-field of the subscale facility. Figure 3 shows that the seven microphones were placed at approximately 228 altitude diffuser exit diameters away, i.e. $r/D_{DE} \sim 228$. The vector in Figure 3 indicates the diffuser exit and flow direction relative to the microphones. Two additional microphones were placed at nearly half the distance ($r/D_{DE} \sim 109$) of the first arc on 45 and 90-degree nozzle aft directivity angles. The microphones had a reported accuracy of +/- 0.2 dB for frequencies between 10 and 4000 Hz.

The microphone data was sampled at a rate of 43 kHz and then filtered using a band-pass, 3rd order, Butterworth filter with cutoff frequencies of 1 Hz and 20 kHz. The microphone data were processed using a Lab-View based Fast Fourier Transform (FFT) acoustic code that was developed in-house and has been used previously on other NASA-SSC test programs. The Lab-View code could provide time-averaged or transient one-octave, 1/3 octave or narrow-band spectra for each microphone. The results in this paper all show the one-octave averaged spectra averaged over the 3-second rocket hot-fire test duration. The acoustic data acquired during steam ejector startup and shutdown have been removed from the time data in order to capture only the nominal 100% power-level facility operation. Several acoustic tests were conducted for the 100% power-level condition that showed repeatability in the measurements to be within +/- 0.5 dB.

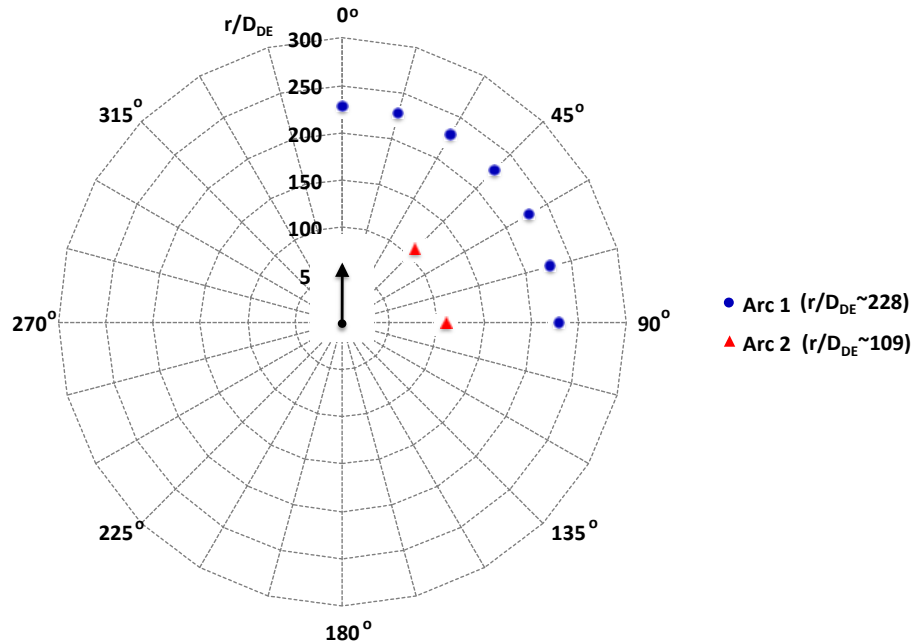


Figure 3: Placement of Microphone Sensors for Far-field Acoustic Mapping of SDT

III. Acoustic Mitigation Approach and Test Matrix

A series of tests were conducted to determine the optimum configuration of a water injection/spray system for lowering the acoustic intensity of the SDT diffuser jet noise. A water-injection ring (shown in Figure 4) was designed and installed during the current test series, where several geometric and dynamic water injection parameters could be varied and the effects on the acoustic environment could be measured. The primary acoustic mitigation parameters investigated were the size/number of water injection holes, the axial location of water injection relative to the SDT diffuser exit plane, angle of water injection relative to the plume exhaust flow direction, and the water flow rate. A summary of the geometric configurations tested has been provided in Table 2. In this report, the nomenclature is that a positive axial placement of the water injection (i.e. $x/D_{DE} > 0$) is downstream of the SDT diffuser exit and a negative x/D_{DE} value indicates the water injection is upstream of the SDT diffuser exit. Also, a 90-degree injection of water is where the water is being injected normal to the plume axis, i.e. normal to the plume's primary flow direction.

Table 3 shows a listing of the range of water flowrates tested during this program and their relation to the total flowrate exiting the SDT diffuser, which is the combined flow from the rocket gas and the 1st and 2nd steam ejectors. It should be noted here that the water was injected through sharp-edged orifices. No special spray nozzles were designed. Also, the two water jet diameters tested (1/4 inch and 1/8 inch) were done in such a way that for each water mass flow rate tested, the two water jet configurations produced the same momentum flux ratio (J) as shown in Table 3. This was done to isolate the mass flow ratio as the critical flow parameter and allow direct comparison between the 1/4 inch and 1/8-inch jets.

Each test series was composed of a facility test firing of the steam generators for 180-second duration. During that time period, the SDT thruster (J-2X subscale engine) was fired three times for 5 seconds each. For all tests, the first firing of the SDT thruster was done with no water injection. The next two firings were with different water injection pressures and flow rates. Performing the tests in this manner ensured that each test had an "acoustic baseline" built into the data set. This allowed a valid comparison of the changes in sound pressure levels between test series due to the water injection under various acoustic mitigation parameters.

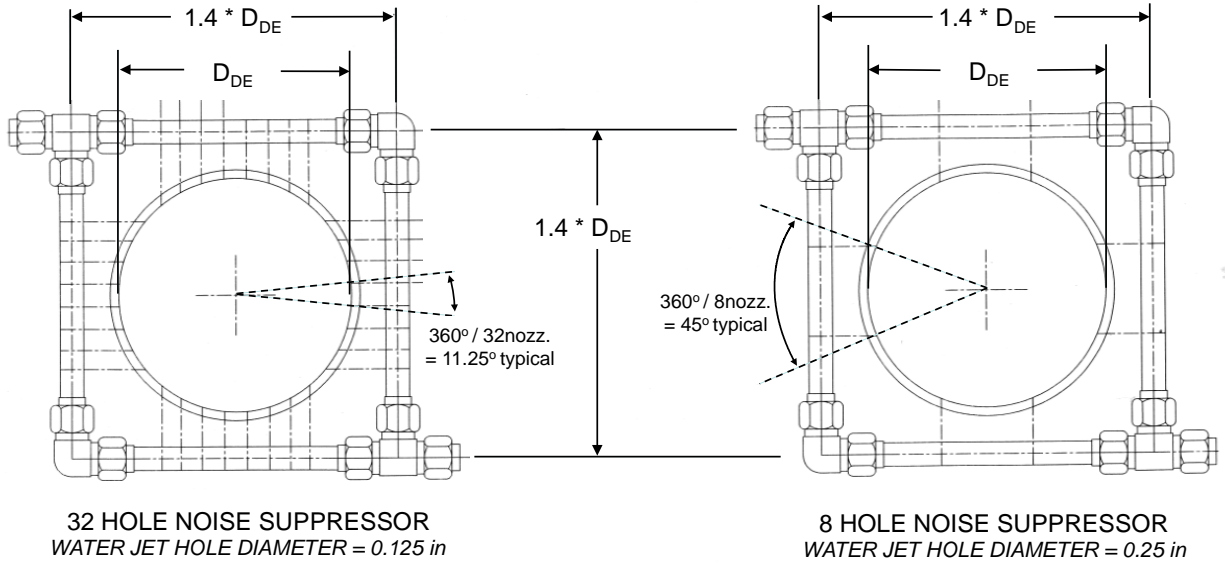


Figure 4: Cross-Sectional Schematics of the Water Injection Noise Suppressors Surrounding the SDT Diffuser Exit Duct

Table 2: Test Matrix of Water Injection Geometric Configurations

| Axial Location (x/D_{DE}) | Hole Diameter (in) | # Holes | Injection Angle Relative to Plume Axis (deg) |
|-------------------------------|--------------------|---------|--|
| +0.5 | 1/8 | 32 | 60 |
| +0.5 | 1/8 | 32 | 90 (normal to plume) |
| +0.2 | 1/8 | 32 | 30 |
| +0.2 | 1/8 | 32 | 60 |
| +0.2 | 1/8 | 32 | 90 (normal to plume) |
| -0.1 | 1/8 | 32 | 30 |
| -0.1 | 1/8 | 32 | 60 |
| -0.1 | 1/4 | 8 | 30 |
| -0.1 | 1/4 | 8 | 60 |
| -1 | 1/4 | 8 | 60 |
| -1 | 1/4 | 8 | 60 |
| -1 | 1/4 | 8 | 30 |
| -1 | 1/8 | 32 | 60 |
| -1 | 1/8 | 32 | 30 |

Table 3: Water-Injection Suppressor Operating Conditions

| Ratio of Total Water-Injection to Total Altitude Diffuser Mass Flow Rate (W_{WJ}/W_{SDT}) | Mass Flow Ratio of a Single Water Jet to Altitude Diffuser Exhaust Jet (W_{WJ}/W_{SDT}) | | Momentum Flux Ratio of a Single Water Jet to Altitude Diffuser Exhaust Jet ($J = \rho_{WJ} * V_{WJ}^2 / \rho_{SDT} * V_{SDT}^2$) | |
|---|---|---------------------------------|--|---------------------------------|
| | $D_{WJ} = 0.125$ in, 32 injectors | $D_{WJ} = 0.25$ in, 8 injectors | $D_{WJ} = 0.125$ in, 32 injectors | $D_{WJ} = 0.25$ in, 8 injectors |
| 0.63 | 0.020 | 0.079 | 0.40 | 0.40 |
| 0.82 | 0.025 | 0.103 | 0.68 | 0.68 |
| 0.92 | 0.029 | 0.115 | 0.86 | 0.86 |
| 1.05 | 0.033 | 0.131 | 1.12 | 1.12 |

IV. Results and Discussions

The angle of water injection relative to the SDT exhaust plume was varied from 30° to 90° to test the sensitivity in reducing the jet noise. Figure 5 shows flow visualizations of the water being injected into the exhaust plume flow at a location of $x/D_{DE}=+0.2$ downstream of the nozzle exit plane. These test configurations consisted of 32 injection holes each with a diameter of 1/8 inch. Upon processing the SDT acoustic mitigation data, the results showed that an increase in the water injection angle relative to the plume exhaust resulted in an improved reduction in the overall sound pressure levels. This behavior is demonstrated in Figure 6, where an increase in injection angle from 30° to 90° (which is normal to plume) resulted in up to approximately 2.5 to 3dB reductions for two water flow rates tested. Therefore, orienting the water injection in a more normal direction such that it produced a larger penetration into the SDT plume resulted in a decrease in the overall acoustic emissions. This trend is consistent with findings reported in other water noise mitigation studies documented in the literature, where the mechanism of reducing the plume noise was presumed to be to reducing the turbulent kinetic energy and velocity fluctuations in the plume shear layer. Figure 6 also shows that for this test configuration an increase in the amount of water injected resulted in greater reductions in the overall sound levels. However, it will be discussed in the following section, that this observed trend was not always the case due to an adverse dynamic coupling with the diffuser operability.

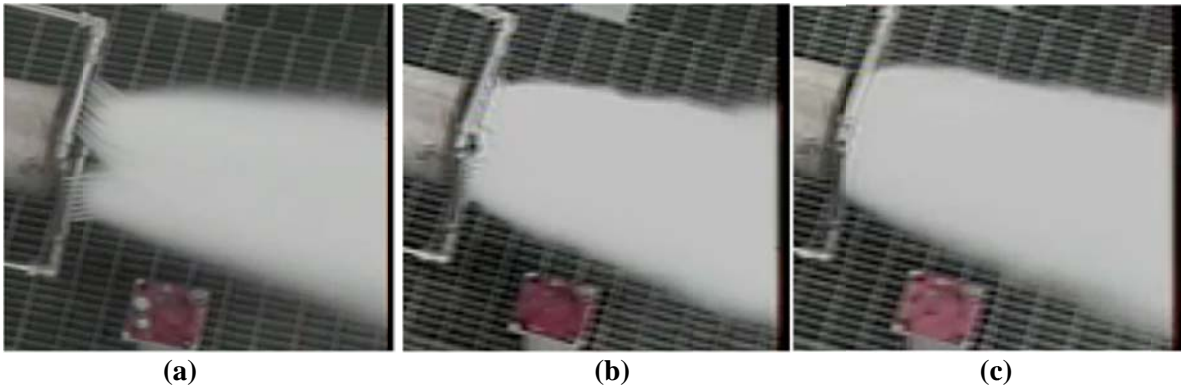


Figure 5: Flow Visualization of 1/8-inch Diameter Water Jet Injection (Qty. 32) at $x/D_{DE}=+0.2$ Downstream of SDT Exhaust Plane for Injection Angles of (a) 30° , (b) 60° and (c) 90°

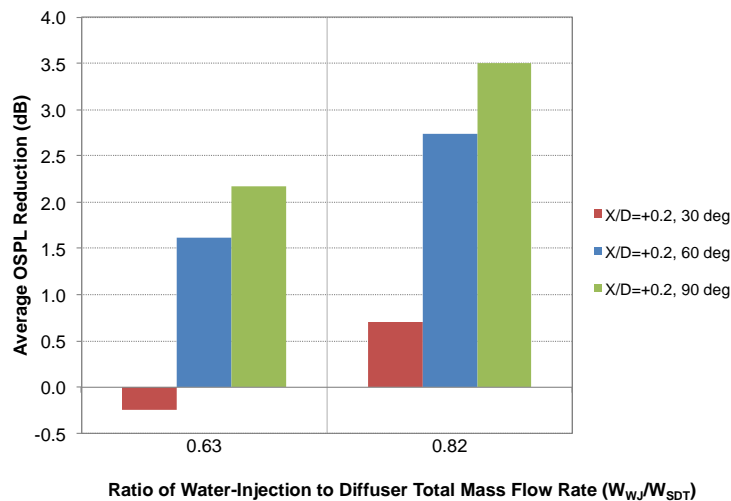


Figure 6: Average OSPL Reduction as Function of Water Flow Rate for 3 Water Injection Angles (1/8-inch Diameter Water Jet Injection Holes of Qty. 32)

Additional tests were conducted where the injection of water was moved *upstream* of the SDT exhaust plane to $x/D_{DE}=-0.1$. Figure 7 shows flow visualizations for the two tested water injection angles of 30° and 60° . The 90° angle injection was not tested at this axial placement, as the water would impinge on the diffuser wall in this upstream injection location. Figure 8 reconfirms the conclusion presented earlier from Figure 6 that an increase in the injection angle resulted in improved SDT noise abatement. Increasing the injection angle from 30° to 60° resulted in a 2dB improvement in the noise attenuation, which is comparable to that observed in the $x/D_{DE}=+0.2$ downstream injection data presented in Figure 6. Also, it is evident from the acoustic data presented in Figure 8 that the overall sound pressure level reductions improved with an increase in water flow rates. However, for water mass flow rates above 92% of SDT ($W_{WJ}/W_{SDT}=0.92$), the level of sound reductions actually decreased. A closer examination of the SDT facility test data showed that at these higher flow rates ($W_{WJ}/W_{SDT}=1.05$), the SDT diffuser had become un-started as indicated by an increase in test cell pressure. Ideally, the test cell pressure should be approximately 0.12 psia with the rocket firing, but for both the 30° and 60° highest flow rate injections, the test cell pressure increased to 0.6 and 0.56 psia respectively. Therefore, when the water flow rate is too high and/or the water is injected too close to the diffuser outlet, the diffuser can aerodynamically un-start due to an effective reduction in outlet area (or increase in perceived back pressure) caused by the added water flow. This leads to the conclusion that for reliable system stability and margin, the noise mitigation should be designed to operate well away from this diffuser “un-start” regime.



Figure 7: Flow Visualization of 1/8-inch Diameter Water Jet Injection (Qty. 32) at $x/D_{DE}=-0.1$ Upstream of SDT Exhaust Plane for Injection Angles of (a) 30° and (b) 60°

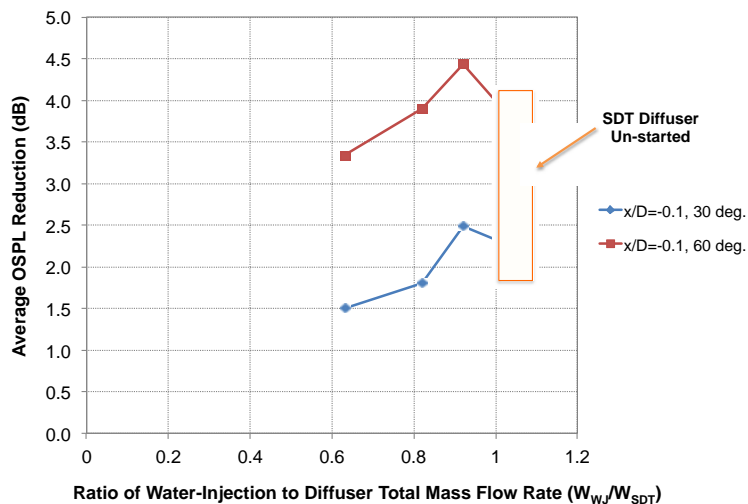
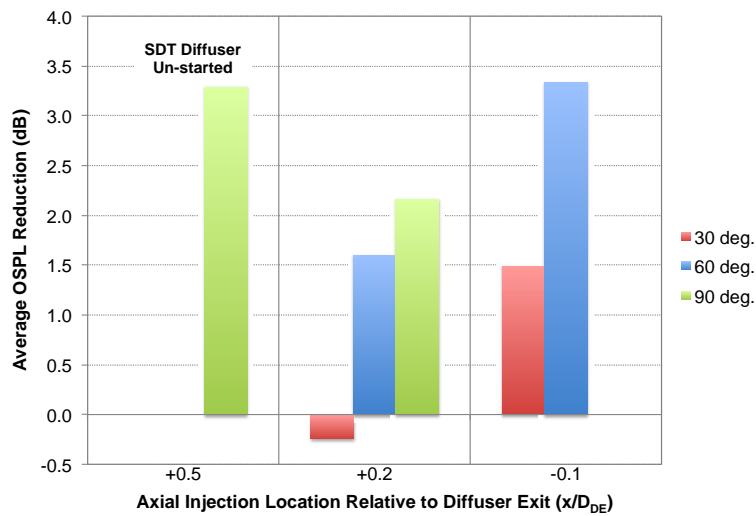
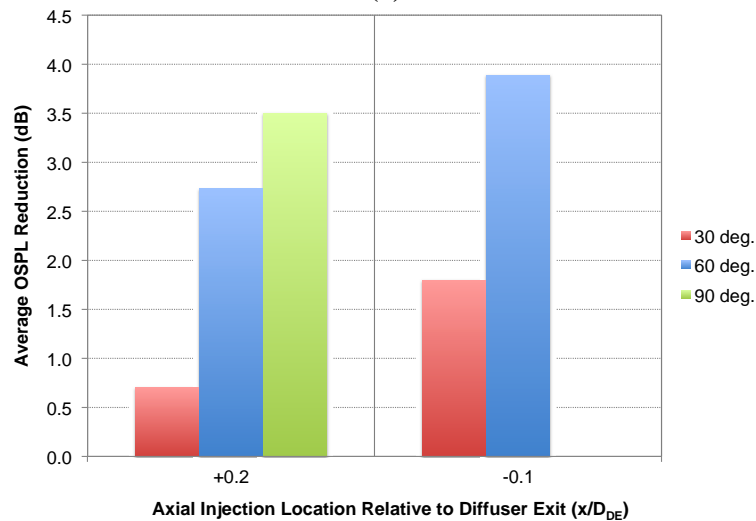


Figure 8: Sensitivity of OSPL Reductions to Water Injection Mass Flow Rate (1/8-inch Diameter Water Jet Injection Holes of Qty. 32)

Another acoustic mitigation design parameter that was investigated in this study was the axial placement of the water injection relative to the exit of the SDT diffuser. As a reminder, the nomenclature is that a positive placement (i.e. $x/D_{DE} > 0$) is downstream of the SDT diffuser exit and a negative x/D_{DE} value indicates the water injection is upstream of the SDT diffuser exit. In all configurations tested except the 90° (normal) water injection angle, improved SDT noise abatement was obtained with more of an upstream injection as demonstrated in Figures 9a and 9b. However, the authors would like to note here that the 90° angle injection at the $x/D_{DE}=+0.5$ axial location did cause a slight increase in test cell pressure from 0.12 to 0.28 psia, thus this data point is invalid as the water injection was affecting the facility performance. Excluding this “un-start” configuration from our data analysis, the improvement with upstream injection placement was observed for both water flow rates tested. It is believed that injecting the water slightly upstream allows the water to attenuate the noise sources at the location of formation (SDT diffuser exit) rather than downstream where the noise sources have already been formed and are producing acoustic disturbances in the environment.



(a)



(b)

Figure 9: Effects of Axial Placement of Water Injection on OSPL Reductions for Normalized Water Flow Rates of (a) 0.63 and (b) 0.82 (1/8-inch Diameter Water Jet Injection Holes of Qty. 32)

The last design variable tested was the size and number of water injection holes. All previous data shown was for a configuration of 32 1/8-inch diameter holes placed around the circumference of the exhaust plume. In the subsequent tests, the injection hole size was increased to 1/4-inch diameter while the number of holes decreased to eight in order to maintain a constant flow rate and momentum ratio. Figure 10 below shows the water injection into the SDT plume for this new configuration at 30° and 60° injection angles. Comparing the flow images in Figure 10 to their counterparts in Figure 7 shows that the water jets produced from the 1/4-inch diameter holes are thicker and spaced further apart as expected. It also appears from these figures that the water jets with the 1/4-inch diameter holes remain more intact over a longer distance, i.e. atomization/vaporization of the 1/4-inch jets are slower. This is also expected, but can play an important role in the interaction of the water jets with the turbulent shear layers of the SDT plume thereby affecting the noise attenuation as will be discussed next.

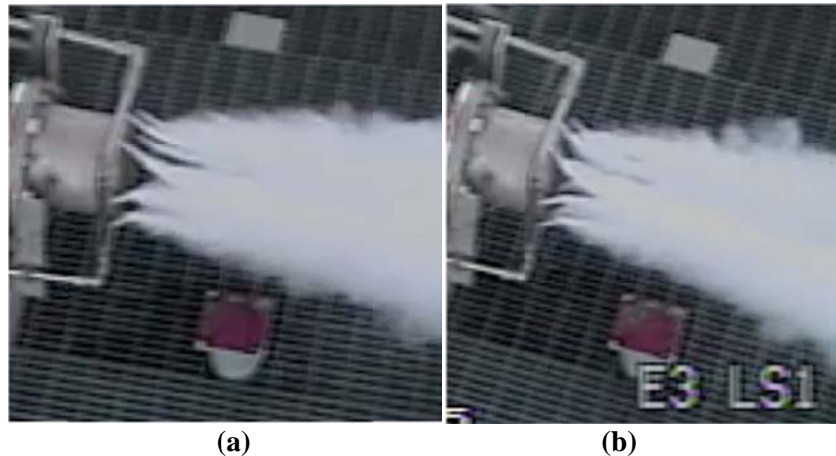
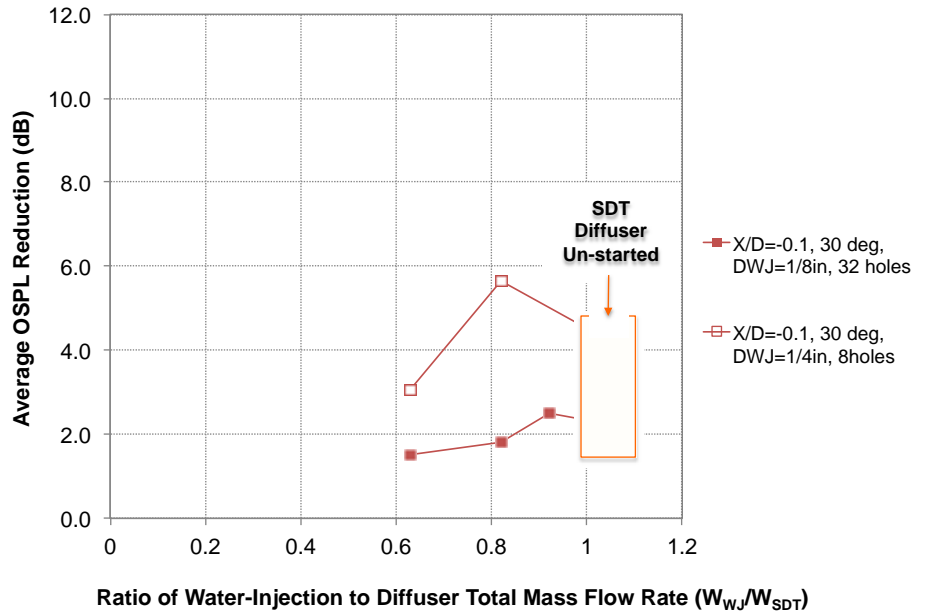


Figure 10: Flow Visualization of 1/4-inch Diameter Water Jet Injection (Qty. 8) at $x/D_{DE}=-0.1$ Upstream of SDT Exhaust Plane for Injection Angles of (a) 30° and (b) 60°

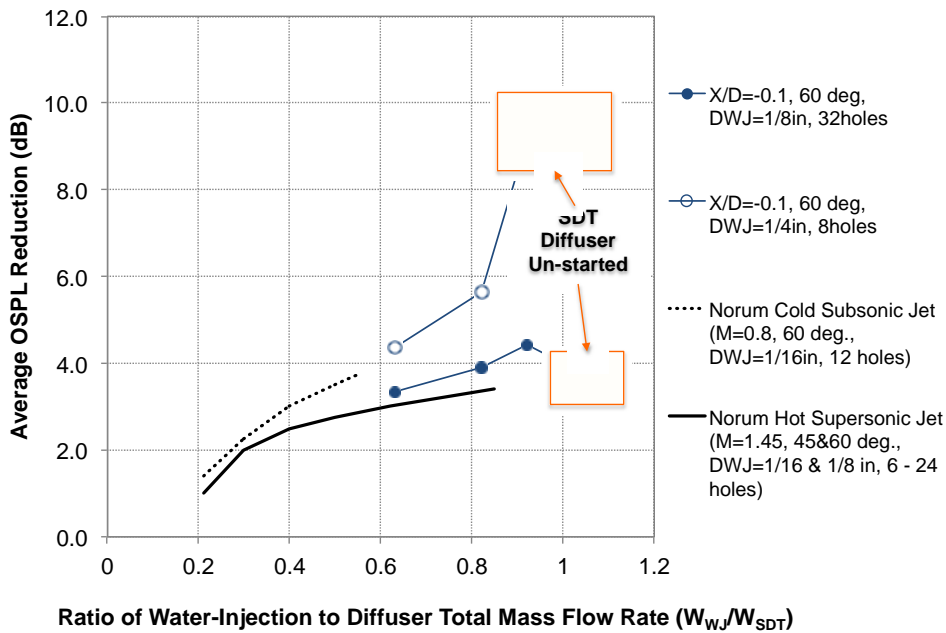
Figure 11 is a plot of the overall sound pressure levels for the 1/4-inch and 1/8-inch diameter water jet configurations. For all cases, the larger water jet diameter configurations showed better reductions in OSPL for the same total flow rate and injection angle. The larger water jet diameter configuration also showed the same general trend as observed previously in the smaller water jet diameter configuration of increased OSPL reductions with increased water flow rate and water injection angle. Preliminary evaluation of Figure 11 suggests almost a 10dB reduction in acoustic noise levels can be obtained with the high flow-rate larger-diameter, water-injection holes. However, additional tests not shown in this figure demonstrated that too large of a water flow rate could result in a SDT diffuser un-start condition. This data is not shown here but occurred at $W_{WJ}/W_{SDT}=0.92$ for the 30° angle injection with 1/4-inch diameter water jets. One discrepancy in the data obtained though is that for configurations with this and larger flow rates, but under a 60° angle injection configuration did not cause an un-started diffuser. This unexpected behavior suggests the possibility of a strong sensitivity or hysteresis characteristic behavior of the SDT diffuser's operability to water injection that might not produce repeatable results. Therefore, the authors are not recommending pursuing the higher flow rates ($W_{WJ}/W_{SDT}>0.82$) for the larger diameter configurations as a viable option unless further repeatability tests are performed.

Lastly, discussion of the acoustic mitigation data would not be complete without a description of the observed behavior of the acoustic spectra under varying the water-injection parameters. Upon review of this data, it was found that attenuation in the acoustic spectra was dependent on all variables tested: water flowrate, angle of injection, axial placement and size/number of injection holes. However, extraction of consistent trends in the data was not obvious due to the complex nature of the data, and in some cases the effects were sufficiently small such that spectra changes were well within the uncertainty

and/or repeatability of the data. In spite of these limitations, a couple of general conclusions can be drawn. First, the water injection affected a wide range of frequencies (>0 to 10kHz) for all test conditions. Secondly, increasing the angle of injection (i.e. to be more normal to the plume flow) produced a greater reduction in the dominant frequency of the noise within the high intensity lobe region (45-degrees). This can be observed by comparing the individual plots in Figure 12. The attenuation of the dominant to low frequency acoustic energy attributes to the previously observed reduction in OSPL with increased angle of water injection.

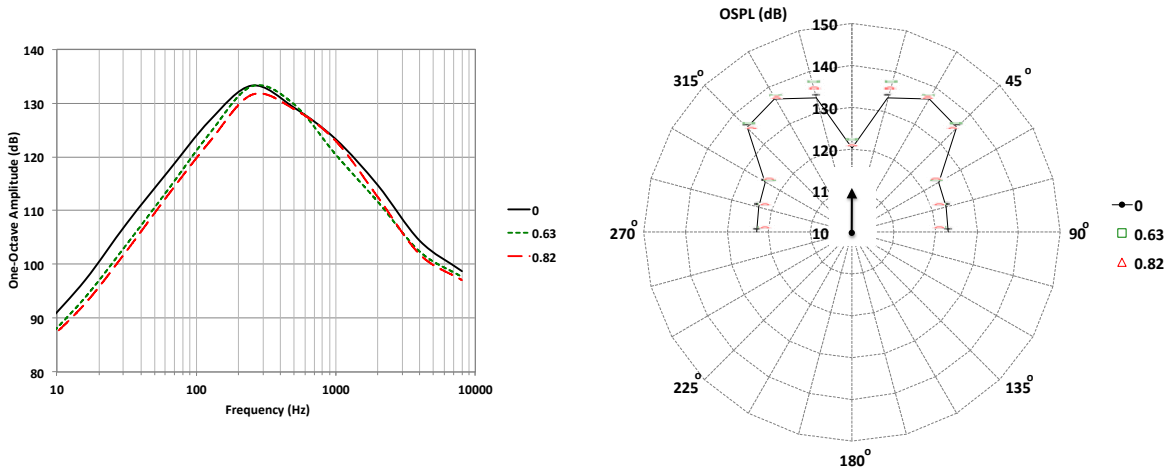


(a)

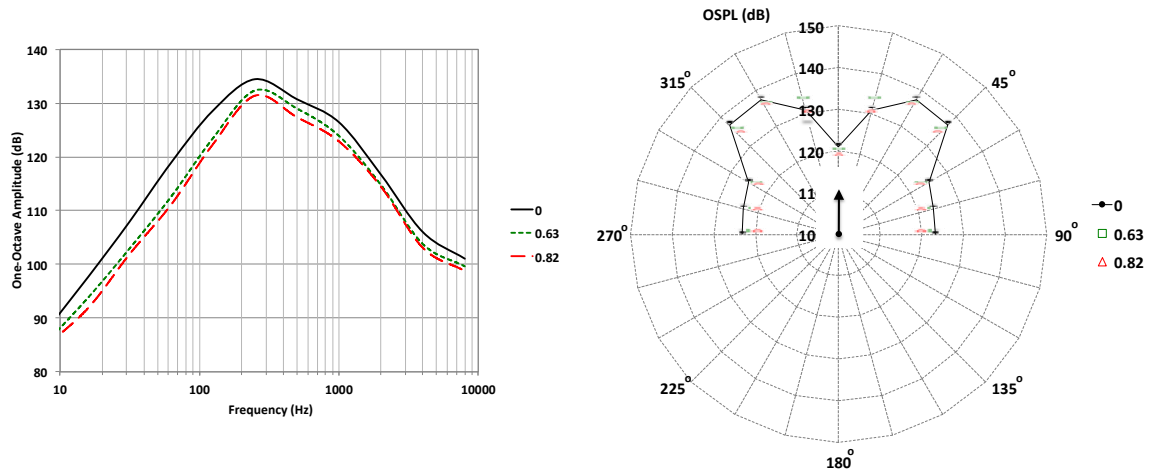


(b)

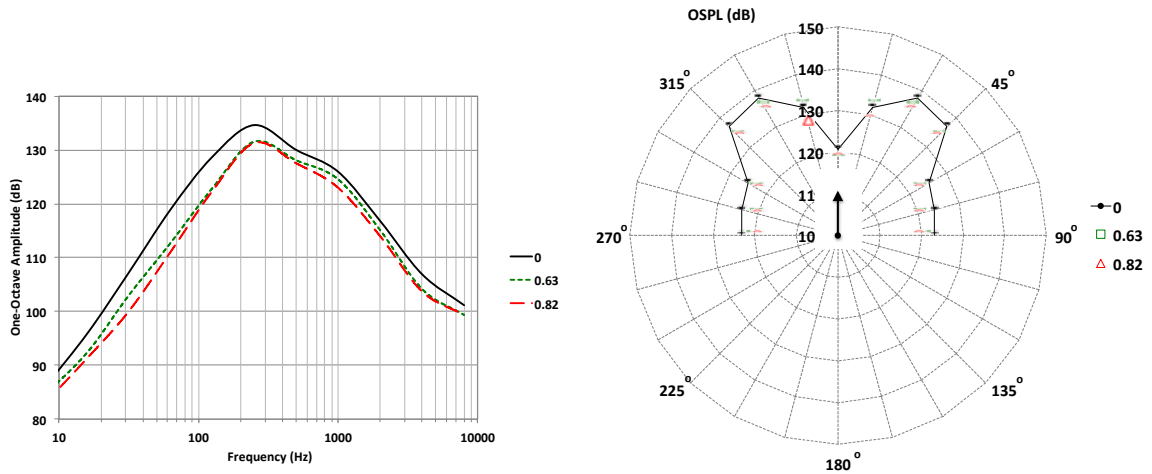
Figure 11: Effects of Water-Injector Size and # of Holes on OSPL Reductions - (a) 30 deg. Injection and (b) 60 deg. Injection



(a)



(b)



(c)

Figure 12: 45° Directivity One-Octave Spectra and OSPL Directivity Plots for $x/D_{DE}=+0.2$ and $D_{WJ}=1/8$ inch Noise Suppressor at Three Different Total Mass Flow Ratios (W_{WJ}/W_{SDT}) of 0, 0.63 and 0.82 (a) 30 deg., (b) 60deg. and (c) 90deg. Injection Angles

V. Conclusion

NASA-SSC was selected as the rocket propulsion test center responsible for development and certification testing of the J-2X upper stage engine at altitude conditions using the new A-3 test facility. Due to mission-criticality of the A-3 facility and uncertainty in its design, a dynamically similar sub-scale test facility was built and tested at the NASA-SSC E-Complex. The focus of this work was to understand the effects of water-injection acoustic mitigation techniques on reducing the “jet-noise” produced by the exhaust of an altitude diffuser of this type. The main noise mitigation technique investigated was a spray of high velocity water injected in the diffuser exhaust plume at different axial locations, impingement angles, and flow rates. The following are the key general conclusions reached in this study:

1. An increase in water injection angle relative to the plume exhaust flow direction resulted in an improved reduction in the overall sound pressure levels.
2. An increase in the amount of water injected relative to the diffuser flow rate resulted in greater reductions in the overall sound levels.
3. Too large of a water flow rate and/or water injected too close to the diffuser outlet resulted in the diffuser aerodynamically un-starting as indicated by an increase in the test-cell pressure. The cause of the diffuser un-start condition was perceived to be due to an effective reduction in outlet area (or increase in perceived back pressure) caused by the added water flow.
4. The results showed significant reductions in noise levels were possible with optimum conditions corresponding to water injection at or just upstream of the exit plane of the diffuser.
5. The larger of the two water jet diameter configurations tested showed better reductions in OSPL for the same flow rates and injection angles.

Acknowledgments

Financial support for the A-3 acoustic mitigation study was provided by the NASA Engineering Safety Center (NESC). The authors would like to thank the NASA NESC-SSC Chief Engineer, Mike Smiles, for his programmatic support. The authors would also like to thank the E-Complex test crew in their support throughout the SDT test program. In addition, this work could not have been accomplished without the acoustic data acquisition support of the SSC Test Technology Lab personnel, W. Mark Mitchell and Brianne Guillot.

References

¹ “Constellation Program: America's Fleet of Next-Generation Launch Vehicles - The Ares V Cargo Launch Vehicle”, FS-2006-07-84-MSFC Pub 8-40599, National Aeronautics and Space Administration, George C. Marshall Space Flight Center, Huntsville, AL 35812.

² “Constellation Program: America's Fleet of Next-Generation Launch Vehicles - The Ares I Crew Launch Vehicle”, FS-2006-07-85-MSFC Pub 8-40598, National Aeronautics and Space Administration, George C. Marshall Space Flight Center, Huntsville, AL 35812.

³ Dumbacher, D., “A New Heavy-Lift Capability for Space Exploration: NASA’s Ares V Cargo Launch Vehicle,” AIAA Space 2006 Conference, San Jose, CA, Sep. 19-21, 2006.

⁴ Allgood, D., Graham, J., Ahuja, V., and Hosangadi, A., “Computational Analyses in Support of Sub-Scale Diffuser Testing for the A-3 Facility – Part I: Steady Predictions,” 45th AIAA Joint Propulsion Conference, Denver, CO, Aug. 2-5, 2009.

⁵ Ahuja, V., Hosangadi, A., Zambon, A., Erwin, J., Allgood, D. and Graham, J., “Computational Analyses in Support of Sub-Scale Diffuser Testing for the A-3 Facility – Part II: Unsteady Analyses and Risk Assessment,” 45th AIAA Joint Propulsion Conference, Denver, CO, Aug. 2-5, 2009.

⁶Allgood, D., Woods, J., Graham, McVay, L. and Langford, L., “Computational Analyses in Support of Sub-Scale Diffuser Testing for the A-3 Facility – Part III: Aero-acoustic Analyses and Experimental Validation,” 45th AIAA Joint Propulsion Conference, Denver, CO, Aug. 2-5, 2009.

⁷Ryan, J. E., Mulkey, C., Raines, N., and Saunder, G. P., “An Overview of the A-3 Subscale Diffuser Test Project,” AIAA 2008-4365, 26th AIAA Aerodynamic Measurement Technology and Ground Testing Conference, Seattle, WA, June 23-26, 2008.

⁸Tam, Christopher K. W., “Supersonic Jet Noise,” *Annual Review of Fluid Mechanics*, Vol. 27, 1995, pp. 17-43.

⁹Krothapalli, A. Venkatakrishnan, L., Lourenco, L., Greshka, B. and Elavarasan, R., “Turbulence and noise suppression of a high-speed jet by water injection,” *Journal of Fluid Mechanics*, Vol. 491, 2003, pp. 131-159, DOI: 10.1017/S0022112003005226.

¹⁰Schlinker, R. H., Reba, R. A., Simonich, J. C., Colonius, T., Gudmundsson, K., Ladeinde, F., “Towards Prediction and Control of Large Scale Turbulent Structure Supersonic Jet Noise,” GT2009-60300, *Proceedings of the ASME Turbo Expo 2009*, Orlando Florida, June 8-12, 2009.

¹¹Jones, Jess H., “Sound Pressure Estimations from a Point Directional Acoustic Source Radiating in an Inhomogeneous Medium”, *Aero-Astrodynamic Res. Review*, No. 3, NASA TM X-53389, October 1965.

¹²“Acoustic Energy Hazards,” *Hazards of Chemical Rockets and Propellants Handbook*, AD 889763, CPIA/194, 1972.

¹³Eldred, K. M., “Acoustic Loads Generated by the Propulsion System”, *NASA Space Vehicle Design Criteria (Structures)*, NASA SP-8072, June 1971.

¹⁴Crocker, M. J. and Potter, R. C., “Acoustic Prediction Methods for Rocket Engines, Including the Effects of Clustered Engines and Deflected Exhaust Flow,” NASA CR-566, 1966.

¹⁵Norum, T. D., “Reductions in Multi-component Jet Noise by Water Injection,” 10th AIAA/CEAS Aeroacoustics Conference, AIAA Paper 2004-2976, Manchester, England, U.K., May 2004.

¹⁶Callender, W., “An Investigation of Innovative Technologies for Reduction of Jet Noise in Medium And High Bypass Turbofan Engines,” PhD Dissertation, University of Cincinnati, 2004.

¹⁷Kandula, M., “Prediction of Turbulent Jet Mixing Noise Reduction by Water Injection,” *AIAA Journal*, Vol. 46, No. 11, November 2008.